SEISMIC PERFORMANCE EVALUATION OF THE BILL EMERSON CABLE-STAYED BRIDGE WITH MEASURED ACCELERATION RECORDS

D.M. Yan[1] and G.D. Chen[2]

[1] *Postdoctoral Fellow, Dept. of Civil, Architectural, and Environmental Engineering, Missouri University of Science and Technology, Missouri, USA, Email: yando@mst.edu*

[2] *Professor, Dept. of Civil, Architectural, and Environmental Engineering, Missouri University of Science and Technology, Missouri, USA, Email:gchen@mst.edu*

ABSTRACT :

A 3D finite element model of the Bill Emerson Cable-stayed Bridge was developed and calibrated with the measured acceleration records taken during the May 1, 2005, earthquake. Under the design earthquake scaled up from the measured rock motions at the bridge site, all cables behave elastically with a safety factor of over 2.35. The two towers behave elastically in-plane. The upper towers above cap beams also remain elastic out-of-plane, but the lower towers approach yielding.

KEYWORDS: Cable-stayed bridge, finite element model, seismic assessment, earthquake records

1. INTRODUCTION

The Bill Emerson Memorial Cable-stayed Bridge opened to traffic on December 13, 2003. It was among the first of its kind to be constructed with 16 longitudinal earthquake shock transfer devices at two towers, six lateral earthquake restrainers, and four tie-down devices at two ends of the cable-stayed span with an additional four pot bearings at the two towers. The bridge is located in a geologically changing area. Due to its critical proximity to the New Madrid Seismic Zone (NMSZ), as well as lack of significant measured ground motions, the Bill Emerson Memorial Cable-stayed Bridge was monitored with a seismic instrumentation system.

The objectives of this study are to (1) develop and validate a realistic FE model of the cable-stayed bridge using recorded ground motions in order to quantify the accuracy of the two simplified models used as ASCE benchmark studies, and (2) validate the design assumptions for critical components such as cables and towers.

2. BRIDGE DATA AND SEISMIC INSTRUMENTATION

2.1. The Bridge Structure

The bridge is a cable-stayed structure spanning the Mississippi River. As schematically shown in Figure 1(a), the final design of the bridge includes two towers, 128 cables, and 12 additional piers in the approach span on the Illinois side. The bridge has a total length of 1206 m, consisting of one 350.6 m long main span, two 142.7 m long side spans, and one 570 m long approach span on the Illinois side. The main span of the bridge provides more than 18.3 m of vertical clearance over the navigation channel. The 12 piers on the approach span have 11 equal spacings of 51.8 m each. Carrying two-way traffic, the bridge has four 3.66 m wide vehicular lanes plus two narrower shoulders.

The total width of the bridge deck is 29.3 m, as shown in Figure 1(b). The deck is composed of two longitudinal built-up steel girders, a longitudinal center strut, transverse floor beams, and precast concrete slabs. A concrete barrier is located in the center of the bridge, and two railings and additional concrete barriers are located along the edges of the deck. The bridge superstructure is directly rested on rock foundation at End Bent 1, and supported on rock through Pier 2. Pier 3 and Pier 4 are supported on two separate caissons. Piers 5 – 12 are supported on pile foundations. Bearings and earthquake devices are vertical and horizontal connections between the superstructure and the substructure of the bridge.

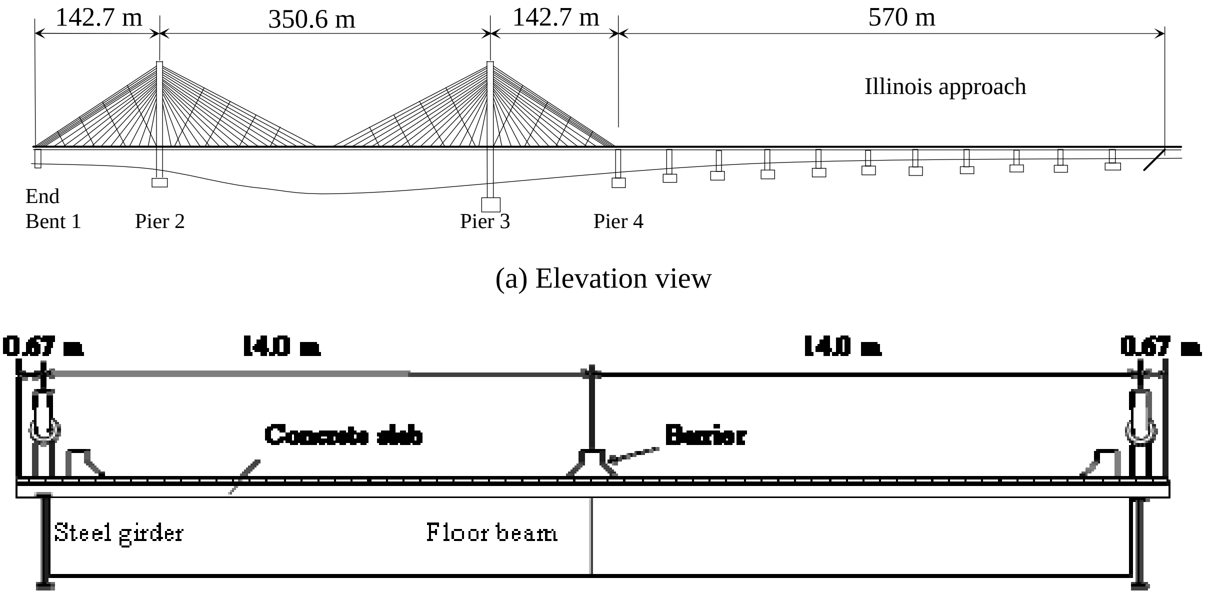

(a) Elevation view

(b) Typical cross section

Figure 1 Schematic view of the Bill Emersion Memorial Cable-stayed Bridge

The bridge is located approximately 80km from New Madrid, Missouri, where three above M8.0 earthquakes occurred (Chen et al., 2005). During the winter of 1811-1812 alone, this seismic region was shaken by a total of more than 2,000 events, over 200 of which were evaluated to have been moderate to large earthquakes. In the past few years, two earthquakes with magnitudes of over 4.0 were recorded in the NMSZ. The cable-stayed bridge structure was proportioned to withstand an M7.5 earthquake (Woodward-Clyde Consultants, 1994).

2.2. Seismic Instrumentation System

The seismic instrumentation system on the bridge consists of a total of 84 Kinemetrics EpiSensor Accelerometers, Q330 digitizers, and Baler units for data concentrator and mass storage (Celebi, 2006). Antennas were installed on two bridge towers at Pier 2 and Pier 3, at free field sites on the Illinois end and on the central recording building near the bridge; wireless communication of data can be initiated among various locations as well as from the bridge and free field sites to the off-structure central recording building.

The accelerometers installed throughout the bridge structure and adjacent free field sites allow the recording of structural vibrations of the bridge and free field motions at the surface and down-hole locations. They were deployed such that the acquired data can be used to understand the overall response and behavior of the cable-stayed bridge, including translational, torsional, rocking, and translational soil-structure interactions at foundation levels. The acquired data can also be used to check seismic design parameters. The monitoring system has been in operation since December 2004. It recorded motions from the May 1, 2005, M4.1 earthquake that occurred at 5.5 km SSE (162^0) from Manila, Arkansas, or 180 kilometers from the bridge. The hypocenter depth was estimated to be approximately 10 kilometers.

3. MODELING OF THE BILL-EMERSON MEMORIAL CABLE-STAYED BRIDGE

3.1. FE Model

A three-dimensional (3-D) finite element (FE) model of the bridge was established based on the geometries and material data from as-built drawings. Frame elements were adopted for girders, floor beams, and the center strut connecting adjacent floor beams. The towers and pile caps were also represented by frame elements. The precast concrete panel/slab was modeled with shell elements. Cables were modeled with cable elements. The sags at the middle of the cables were determined from the bridge drawings. The complete FE model of the entire bridge has a total of 3,075 joints, 3,622 frame elements, 106 shell elements, and 853 2-D solid elements, resulting in 15,926 degrees of freedom.

The elevation difference both in transverse and longitudinal directions due to the designed slope and vertical curve in the bridge deck was taken into account. The bridge has a total of 128 cable stays in its main span. Each cable is attached at one end to the top flange of a composite steel girder and at the other end to the work point of the tower. Both attachment points are away from the neutral axes of their respective supporting structural elements (deck and tower). As such, rigid links were introduced to connect the cables to the girders as shown in Figure 2(a), and to connect the cables to the tower as illustrated in Figure 2(b). The use of rigid links ensures that the theoretical lengths, horizontal angles, and the maximum sag of the cables are exactly the same as designed.

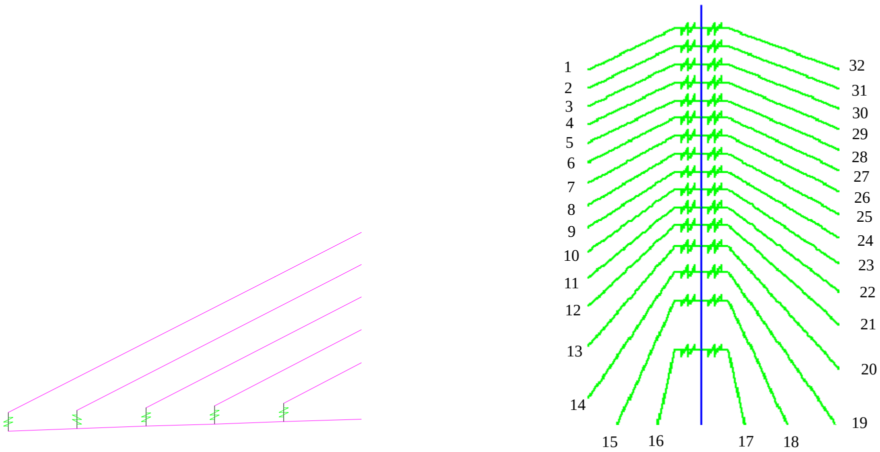

(a) Deck (b) Tower at Pier 2

Figure 2 Details of the Deck and Tower Modeling

A total of 16 6.67 MN shock transmission devices were provided between the towers and the deck. These devices were installed in the longitudinal direction to allow for slow expansion of the deck due to temperature changes. Under dynamic loads, these devices are extremely stiff and are assumed to behave as rigid links. Additionally, earthquake restrainers were employed in the transverse direction between the towers and the deck. At the location of towers, the deck is restrained in the vertical direction. The bearings at Bent 1 and Pier 4 are designed to permit longitudinal displacement and rotation about the transverse and vertical axis.

To simulate the deck-to-tower connections, an approach is employed by attaching elements to separate joints at the same location and constraining their motions with an “Equal” function. The pot bearings used between steel girders and pier cap beams at Piers 2 and 3 were modeled to allow for the longitudinal translation and free rotation about any axis. The earthquake lateral restrainers at the center of the floor beam at End Bent 1, Piers 2 to 4 were modeled to provide lateral restraints between the floor beam and the cap beam. Two earthquake shock transmission devices were modeled as a hinge in the longitudinal direction for seismic analysis.

Since Piers 2 to 4 are either rested on rock or supported on caissons, soil-structure interaction is negligible. As such, these piers were fixed at their bottom ends in the FE model. On the other hand, Piers 5 to 14 in the Illinois Approach are supported on pedestal pile-group foundations. In the FE model, the soil-pile interaction was simulated by linear dashpots and springs in longitudinal (traffic), transverse, and vertical directions, respectively.

3.2 Parametric Analysis

Different estimates of structural and material properties may affect the behaviors of the bridge model. To ensure that the model is robust and reliable, various parameters are perturbed to understand the sensitivity of the model. These parameters include the presence of the approach spans, the soil properties around pile foundation, the bearing restraint, and the mass density of concrete. Since the cable-stayed main span of the bridge is much more flexible than the Illinois approach spans, the first 30 modes of vibration were found sufficient to determine the seismic performance of the main span.

3.2.1 Presence of the approach span of the bridge

In order to understand the effect of approach on the dynamic behavior of the main span, two FE models were run and compared for their dynamic characteristics. One model includes the approach spans, and the other does not. It was observed that, for the first 30 frequencies, the difference in natural frequency is all less than 1.8%. The main bridge almost vibrates independently of the approach spans due mainly to their different characteristics. The maximum difference in frequency corresponds to the transverse vibration.

3.2.2 Pier boundary conditions

The boundary conditions (BC) of bridge piers are usually idealized as fixed, hinged or roller supports in the analysis models (Hu et al., 2006). In the present study, four combinations of support conditions are considered for three piers of the main span, as described in Table 1. Here, a fixed condition means no translational and no rotational motions in all directions; a hinge condition means no translational motions in all directions and no rotational motion about the traffic direction; an expansion condition allows for longitudinal motion along the traffic direction only.

Table 1 Pier Boundary Conditions

Case	Pier 2	Pier 3	Pier 4
1	Fixed	Fixed	Fixed
2	Hinge	Fixed	Hinge
3	Expansion	Fixed	Expansion
4	Hinge	Hinge	Hinge

For various boundary conditions (BC), the calculated frequencies are presented in Figure 3. It can be seen from Figure 3 that Case 1 with fixed supports gives the highest natural frequencies among all four cases, corresponding to a stiff bridge model. Expansion and hinge supports in Cases 3 and 4, respectively, make the bridge more flexible. However, the maximum frequency difference between Case 1 and Case 4 is less than 2%. In this study, Case 1 is used in the following analysis for simplicity and is a good representation of physical conditions as indicated in as-built drawings.

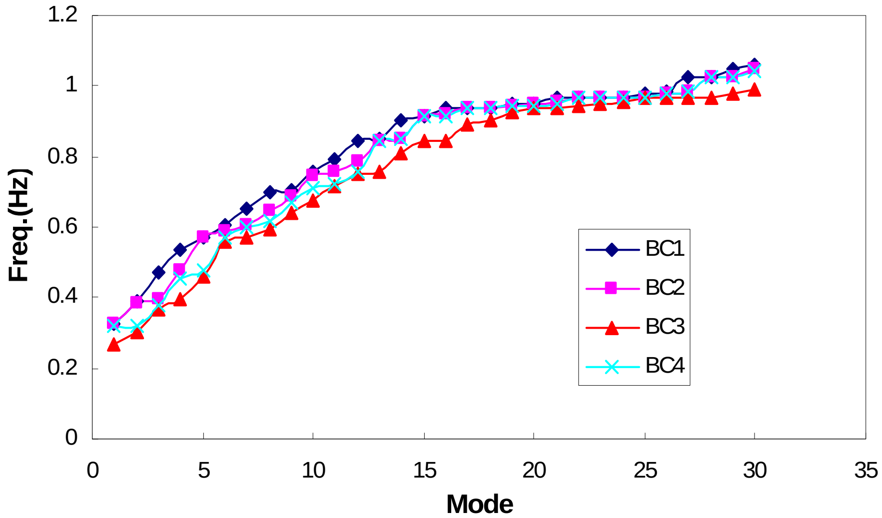

Figure 3 Frequency Variations under Different Boundary Conditions

3.2.3 Influence of pile foundation

Three cases are considered to investigate the effect of pile foundations in the approach spans. The first case is used to model the support of the piers in the approach spans as springs and dashpots in vertical, longitudinal, and traffic directions. This case is supposed to simulate the effect of group pile foundations. The second case is used to fix the bases of all piers to restrain motions in all degrees of freedom. The third case is used to model the bases of piers as hinges. A comparison of the three cases clearly shows that there is basically no difference among the three cases as far as the first 30 natural frequencies are concerned. As explained before, this result is because the first 30 modes mainly involve the vibration of the main bridge or the cable-stayed span. Therefore, the accuracy of foundation modeling is insignificant for the analysis of the cable-stayed span.

4. FE MODEL CALIBRATION

5.1 Calibration by Natural Frequency

The numerically calculated frequencies and the experimentally identified frequencies were compared in Figure 4 for the modes of vibration up to 17.94 Hz. The maximum relative error was found less than 10%. Considering the complexity of the structure, the computed frequency agrees fairly well with the measured data. To understand the difference between the 3-D model and the Spine/C-shape models (Caicedo et al., 2000, Dyke et al., 2003), the calculated frequencies from various models are all compared in Table 2 with the measured frequencies. It is clearly seen that the fundamental frequency of the 3-D model is 7% higher, indicating that the simplified model underestimated the stiffness of the bridge structure due mainly to the neglect of diaphragm actions of the bridge deck. The shapes of the first four dominant modes with significant mass participations were found comparable between the 3-D model and the C-shape model. As pointed out in the study (Caicedo et al., 2000), the spine model is even less accurate. Indeed, the natural frequencies determined by the C-shape model are all closer to those of the 3-D model in this study.

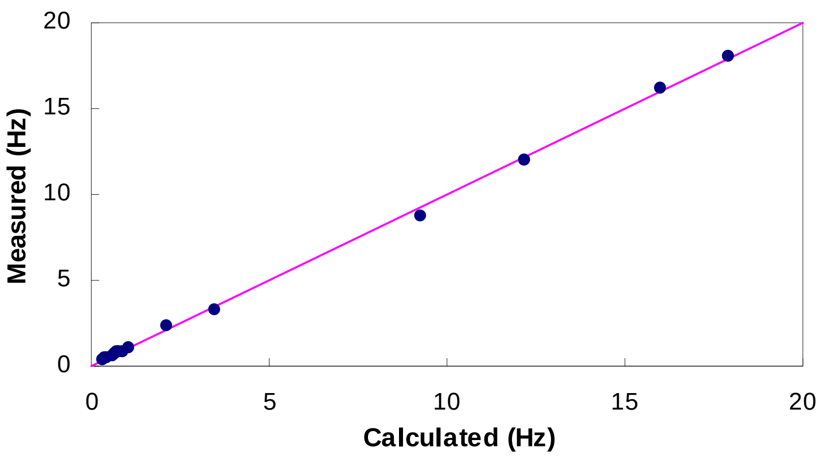

Figure 4 Correlation between the Calculated and the Measured Frequencies

Table 2 Calculated versus Measured Natural Frequencies

No.	FE Model (Hz)	Measured (Hz)	Error (%)	Spine Model (Hz)	C-Shape Model (Hz)
1	0.32	0.34	-4.14	0.2978	0.3034
2	0.39	0.42	-7.76	0.3978	0.3981
3	0.47	0.50	-5.51	0.5264	0.4711
4	0.60	0.59	2.59	0.6575	0.6717
5	0.65	0.65	0.01	0.6772	0.6791
6	0.70	0.71	-2.37	0.7363	0.7029
7	0.75	0.78	-2.67	0.8801	0.7379

5.2 Mode Shape Validation

The 3-D FE model was further validated with the mode shapes of vibration. A good correlation between the calculated and the identified mode shapes of several vibration modes has been demonstrated. To systematically evaluate the correlation of all calculated and identified mode shapes, the modal assurance criterion (MAC) index (Friswell and Mottershead, 1995) is computed for each mode as follows:

$$MAC_{jk} = \frac{(\{\phi_j\}^T\{\phi_k\})^2}{(\{\phi_j\}^T\{\phi_j\})(\{\phi_k\}^T\{\phi_k\})} \tag{1}$$

where $\{\phi_j\}$ is the j^{th} mode shape from the FE model and $\{\phi_k\}$ is the k^{th} mode shape identified from the measured accelerations. In this study, the mode shapes are extracted from the seismic records during the earthquake. Due to limited numbers of accelerometers installed on the approach span, only the cable-stayed main span of the bridge is considered. In addition, the exact locations of accelerometers are unknown. The mode shapes identified from the acceleration records are approximate. This estimation may cause some uncertainties in the measured mode shapes. The MAC values of the 1st, 2nd, and 3rd modes are 0.976, 0.837 and 0.950 respectively. The calculated mode shapes correlate well with the identified mode shapes.

5. SEISMIC PERFORMANCE EVALUATION OF THE BRIDGE

The measured earthquake records generally reflect the regional geologic conditions and related characteristics of the seismic zone. The ground motions during the May 1, 2005 earthquake at bottom of Pier 2 were recorded on rock. They were scaled up by 10,000 times to approximately represent an M7.5 design earthquake for the bridge. The peak acceleration of the modified rock motions reaches 0.57g in transverse and longitudinal directions and 0.42g in the vertical direction. They have wide frequency ranges with a dominant frequency of approximately 10 Hz. The amplified three-component rock motions will be used as inputs to the FE model of the cable-stayed bridge to assess the structural conditions of main components.

Considering their critical role in maintaining the structural integrity of the bridge, two towers and two cables were evaluated. Time history analysis was conducted to characterize the stress distribution on towers. To mimic the actual excitation condition, the 3-D FE of the cable-stayed bridge was subject to the amplified rock motions in three directions simultaneously. Normally, the maximum moment would possibly occur at the bottoms of the two towers and at the intersections of tower columns and cap beams.

To determine the bending capacity of each section of the towers, moment curvature analysis was performed to evaluate the load-deformation behavior of a reinforced concrete section, using the nonlinear stress-strain relationships of concrete and steel materials. In this study, the Whitney stress block for concrete along with an elasto-plastic reinforcing steel behavior was used as discussed in Wang (2007).

After the bending moment demands are determined from the FE model of the bridge, the capacity over demand ratio of each column can be evaluated. The ratios of the bending capacity to the maximum moment range from 1.12 to 2.17 (out-of-plane bending), and from 1.87 to 3.66 (in-plane bending). For both top and bottom sections of the two towers, the capacity over demand ratios corresponding to the moments are all above 1.1. In fact, all the in-plane seismic moments are significantly less than their yield moments of corresponding sections, indicating an elastic behavior of the bridge or a conservative design for earthquake loads. Only the out-of-plane bending at the bottom section of Pier 3 is near yielding.

The maximum stresses of all stay cables induced by dead plus earthquake loads are calculated. The ratios of design stress to maximum calculated stress and the material strength to maximum calculated stress are presented in Figure 5. It is observed that most design stresses are close to the maximum tensile stresses during a design earthquake. As indicated by Figure 5, all stay cables are in elastic range under the dead plus earthquake loads. The factor of safety is over 2.78, which ensures the safety of the bridge during a design earthquake. The assignment of cable numbers is referred to Figure 2(b).

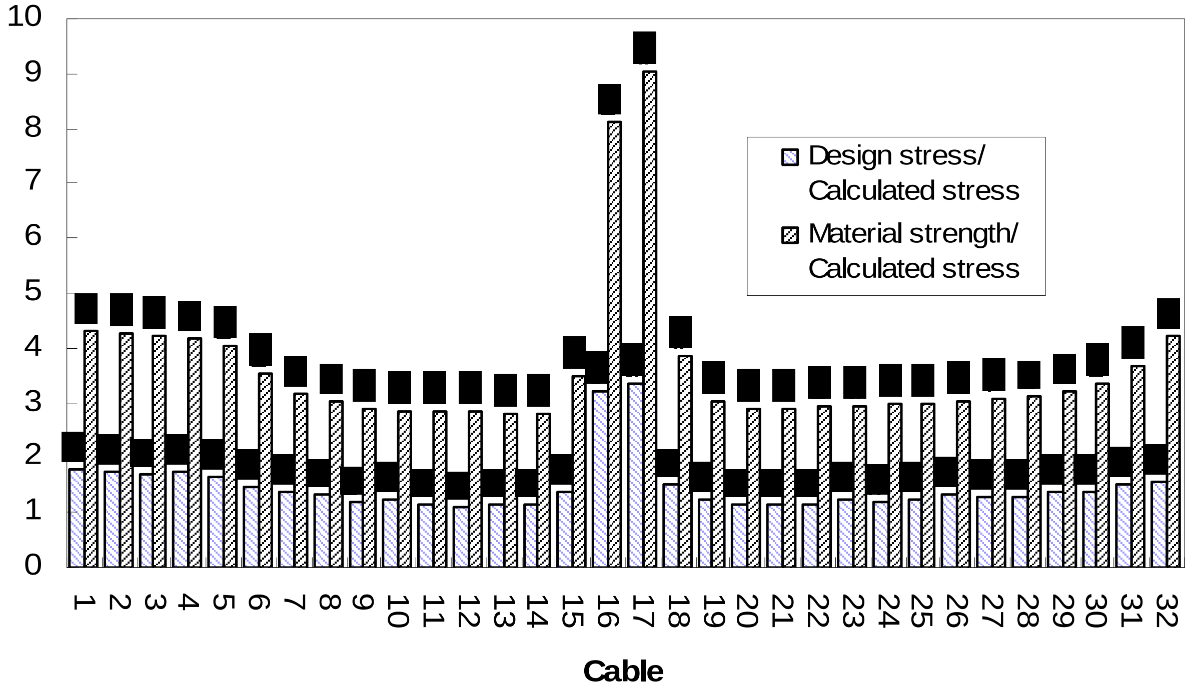

Figure 5 Factor of Safety of All Cable Stays

Figure 5 also indicates that Cable 14 experienced the largest stress during the earthquake. The stress time history in this cable is presented in Figure 6. The initial stress at the beginning of the earthquake represents the dead load effect, approximately 550MPa. This means that the earthquake effect is approximately 669-551=118 MPa, which accounts for 22% of the dead load stress. It was also found that the minimum stress during the earthquake is approximately 102MPa, indicating that the cable is always in tension.

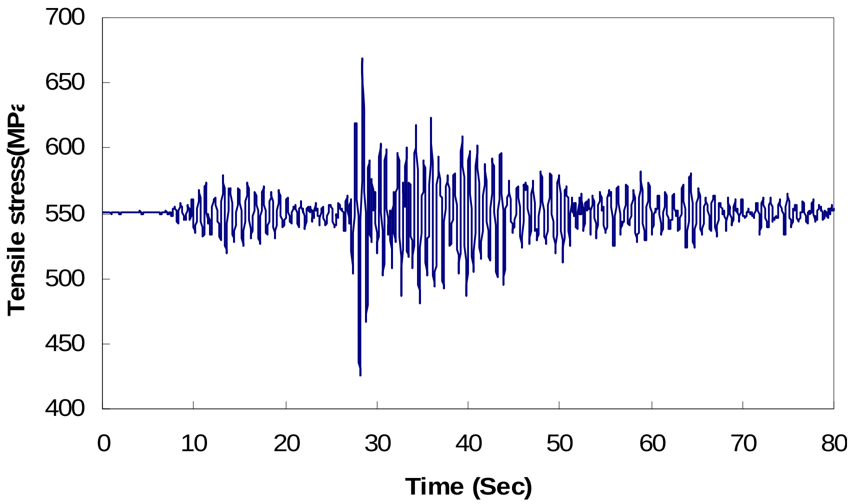

Figure 6 Time History of Tensile Stress in Cable 14

6. CONCLUDING REMARKS

Based on extensive analyses of the bridge model, the following main observations can be made:

1. The 3D model that has been developed and validated with the measured responses indicated that the two

simplified models used in the literature significantly underestimate the effects of bridge diaphragms.

2. The computed natural frequencies of the 3-D FE model agree fairly well with those from the field measured data. The maximum error of the first 16 significant modes is less than 10%. The mode assurance criterion index between a computed mode shape and its corresponding measured one is above 0.837 for the first three modes, indicating a general agreement between the two.

3. All cables remain in tension and behavior elastically under a postulated design earthquake with a factor of safety greater than 2.35. The two H-shaped towers always remain in elastic range with a wide margin of safety except that their bases are near yielding out of plane under the design earthquake.

7. ACKNOWLEDGEMENTS

Financial support to complete this study was provided in part by the Missouri Department of Transportation and the U.S. Department of Transportation under the auspices of Center for Transportation Infrastructure and Safety, a National University Transportation Center at Missouri University of Science and Technology. The results and opinions expressed in this paper are those of the authors only and do not necessarily reflect those of the sponsors. A special thank goes to Dr. M. Celebi from the United States Geological Survey for his assistance in retrieving the earthquake records from the May 1, 2005, earthquake event.

REFERENCES

Celebi, M. (2006). Real-time seismic monitoring of the new Cape Girardeau Bridge and preliminary analysis of recorded data: an overview. *Earthquake Spectra* **22:3**, 609-630.

Chen, G.D., Anderson, N., Luna, R., Stephenson, R.W., El-Engebawy, M., Silva, P.F., and Zoughi, R. (2005). Earthquake hazards assessment and mitigation: a pilot study in the New Madrid Seismic Zone. CIES Technical Report 07-073, Center for Infrastructure Engineering Studies (CIES), Submitted to FHWA Turner-Fairbanks Highway Research Center.

Caicedo J. M., Turan, G. and Dyke S.J., et al. (2000). Comparison of modeling techniques for dynamic analysis of a cable-stayed bridge. Proceedings of the 2000 ASCE Engineering Mechanics Specialty Conference (CD-Rom), Austin, Texas.

Dyke S.J., Carcedo J.M. and Turan G., et al. (2003). Phase I benchmark control problem for seismic response of cable-stayed bridges. *ASCE Journal of Structural Engineering*, 857-872.

Friswell M.I. & Mottershead, J.E. (1995). Finite Element Model Updating in Structural Dynamics. Dordrecht, Netherlands, Kluwer Academic Publishers.

Hu J.D., Harik Issam E., Smith S.W., Campbell J. Gagel, J.E. and Graves R.C. (2006). Baseline modeling of the Owensboro cable-stayed bridge over the Ohio River. Research Report KTC-06-04/FRT116-020-1F, College of Engineering, University of Kentucky.

Wang W. (2007). Structural condition assessment of the Bill Emerson Memorial Cable-Stayed Bridge using neural networks. Doctoral Dissertation, University of Missouri-Rolla.

Woodward-Clyde Consultants. (1994). Geotechnical seismic evaluation of proposed new Mississippi River Bridge (A-5076), Cape Girardeau, Missouri. Report No. 93C8036-500.